

## <sup>a</sup>Radiation pattern and impurity transport in impurity seeded ELMy H-mode discharges in JET.

M.E. Puiatti<sup>1</sup>, G. Telesca<sup>1</sup>, J. Rapp<sup>2</sup>, M. Mattioli<sup>1</sup>, P. Monier-Garbet<sup>3</sup>, M. Valisa<sup>1</sup>, I. Coffey<sup>4</sup>, P. Dumortier<sup>5</sup>, C. Giroud<sup>3</sup>, L.C. Ingesson<sup>6</sup>, K.D. Lawson<sup>7</sup>, G. Maddison<sup>7</sup>, A.M. Messiaen<sup>5</sup>, A. Murari<sup>1</sup>, M.F.F. Nave<sup>8</sup>, J. Ongena<sup>5</sup>, J. Strachan<sup>9</sup>, B. Unterberg<sup>2</sup>, D. Van Eester<sup>5</sup>, M. von Hellermann<sup>6</sup> and contributors to the EFDA-JET workprogramme<sup>a</sup>

<sup>1</sup>Associazione Euratom-ENEA sulla Fusione, Consorzio RFX, Padova, Italy

<sup>2</sup>Institut für Plasmaphysik, Forschungszentrum Jülich GmbH, Jülich, Germany

<sup>3</sup>Association Euratom-CEA, DRFC, CEA Cadarache, St Paul lez Durance, France

<sup>4</sup>Queens University, Belfast BT7 INN, North Ireland

<sup>5</sup>LPP-ERM/KMS Euratom-Belgian State Association, Brussels, Belgium

<sup>6</sup>FOM Instituut voor Plasmafysica Rijnhuizen, EURATOM Association, Nieuwegein, The Netherlands

<sup>7</sup>EURATOM/UKAEA Fusion Association, Culham Science Center, Abingdon, UK

<sup>8</sup>Associação Euratom-IST, Centro de Fusão Nuclear, Lisboa, Portugal

<sup>9</sup>Princeton Plasma Physics Laboratory, USA

**Introduction** In JET, the injection of argon simultaneously with deuterium in ELMy H-mode discharges has allowed the achievement of high confinement ( $H_{97} \approx 1$ ) at high density ( $n_e/n_{Gr} \geq 1$ ) in various experimental scenarios [1]. The motivation of this paper is to characterize different plasma configurations with respect to the equilibrium between highly radiative regimes and increase of medium-Z impurity ions in the centre in long lasting discharges. The study of the impurity behaviour allows the identification of high performance regimes with hollow radiation profiles and without impurity accumulation.

**Impurity seeding and radiative mantle** An immediate way to compare the radiation profile evolution in different discharges is to observe the time behaviour of the ratio between the value of the radiated power (as obtained from the Abel inversion of the bolometric data) at the plasma centre and at the edge (maximum value). This ratio is drawn in fig. 1 for four different experimental situations : in shot #52136 (septum, low  $\delta$ , NBI heating) it increases continuously during the after-puff phase (i.e. the phase immediately following  $D_2$  and Ar puffing, from 59s to 62s in this case), corresponding to a peaking of the radiation profiles ; a similar behaviour is observed (though not shown in the figure) for the high  $\delta$ , ITER-like configuration shot #52152. Therefore, although very high densities ( $n_e/n_{Gr} \geq 1$ ) and high confinements ( $H_{97} \sim 1$ ) are reached at rather high values of the ratio  $\Gamma = P_{rad}/P_{in} \sim 60\%$  and relatively low

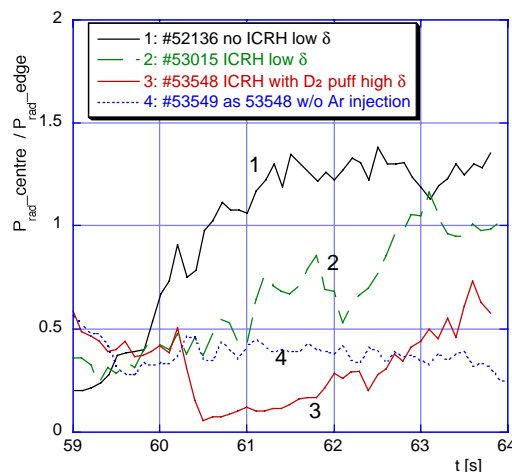


Fig. 1 : Ratio between the radiated power at the plasma centre and the maximum value at the plasma edge

<sup>a</sup> appendix of J.Pamela, Overview of recent JET results Proc. of IAEA Conf., Sorrento 2000

$Z_{\text{eff}}(\leq 2)$  an edge radiative mantle may not be recognized. A different behaviour is observed in shot #53015, in which  $\sim 2\text{MW}$  of ICRH power are added on top of 12 MW of NB power [2]. The level of puffed Ar is higher than in shot #52136, but a quasi-steady state phase with about constant ratio between the central and external radiation is reached, though at lower  $\Gamma \sim 50\%$ . The latter behavior may be associated to the ICRF power deposition profile, that is quite peaked in a narrow volume around the central resonant layer. The ICRH hampers the central plasma cooling normally observed in the after-puff phase and consequently prevents a further increase of the radiation from the central plasma.

In shots like #53146 or #53548, characterized by a high  $\delta$  and continuum deuterium puff throughout the whole discharge (i.e. without an after-puff phase) and with 1.5 MW ICRH added to the NBI, when the argon injection starts (at 60s), the edge radiation increases with respect to the central one. To underline the effect of Ar injection, a reference discharge without seeding is also drawn in fig1.

**Impurity transport** The impurity (intrinsic and injected) transport in the discharges shown in fig.1 has been simulated by a 1-D time dependent impurity diffusion model coupled to an atomic collisional-radiative code [3], where the radial impurity ion flux  $\Gamma_z$  is expressed in terms of a diffusion coefficient  $D$  and a pinch velocity  $v$  ( $v > 0$  corresponds to inward velocity):

$$\Gamma_z(r) = -D(r) \frac{\partial n_z(r)}{\partial r} - v(r) n_z(r).$$

The experimental  $T_e$  and  $n_e$  profiles are assumed as input to the code, while the argon influx is determined by reproducing an Ar VII (585) or Ar XV (221) line evolution.

To simulate the low triangularity septum discharge (#52136), at the start of the after-puff phase, a pinch velocity inward directed in the central region and increasing in time must be assumed, as shown in fig.2, with a diffusion coefficient decreasing towards the plasma centre. These profiles of the transport parameters allow the reconstruction of the Ar XVI, Ar XV and central soft X-rays time evolution, of the plasma effective charge ( $\sim 1.8$ ), of the total radiation profiles and of the emission spectra measured in the range 20-40 and 140-450. The resulting profiles of Ar ions are strongly peaked in the centre, as shown in fig.3. A strong Ar peaking is also observed by charge-exchange measurements: the profiles of the stripped ion are consistent with the simulation, also if it has to be mentioned that in absolute terms the simulated  $\text{Ar}^{18+}$  density is lower than the measured one by a factor of two. An edge diffusion barrier must be considered ( $D$  decreasing at the edge), as previously found [2], to approach the high experimental value

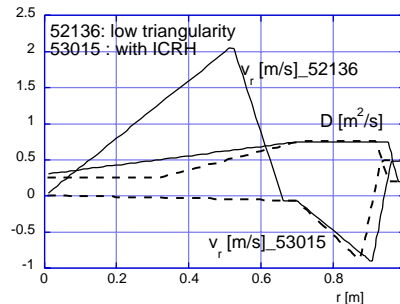


Fig.2 : Diffusion coefficient and pinch velocity for shots #52136 and #53015 at  $t=60\text{s}$

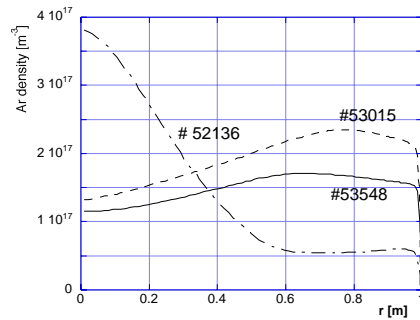


Fig. 3 : Radial profile of Ar density

of the ratio  $\rho$  between the C VI Ly $\alpha$  and the C V resonance lines ( $\rho \sim 4$ ). Carbon profiles, differently from Ar, do not show a peaking in the centre. The analysis of the

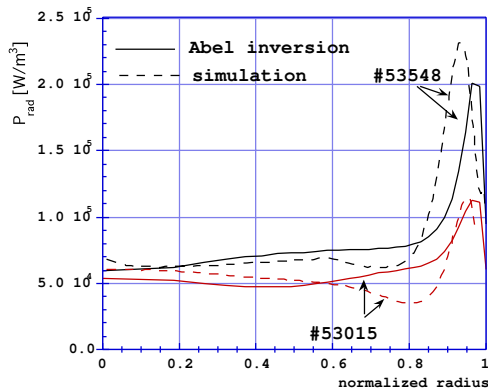


Fig. 4 : Radial profile of the radiated power density during the quasi-stationary high confinement phase for shots #53015 ( $t=61$  s) and #53548 ( $t=62$  s)

ITER-like shot #52152 leads to similar conclusions in terms of argon transport and accumulation. Instead, a different impurity transport scenario is found for shot #53015. In this case, while the diffusion coefficient remains substantially unchanged, the simulation requires a pinch velocity quite lower than in #52136, initially outward directed along the whole minor radius (fig.2), and in a later phase slightly inward in the central region, to account for a slow peaking process of the radiated power (fig.4). The resulting Ar density profile is slightly hollow or quite flat, as drawn in fig.3, and carbon profile is hollow and consistent with that from CX measurements. Therefore the application of ICRH appears to be beneficial to limit the argon penetration and to the establishment of an hollow radiation profile, possibly through the maintenance of sawteeth, as reported in another paper [2]. It should be mentioned that shots #52136 and #53015 have also different fluxes of deuterium and argon: while in #52136 during the after-puff both argon and deuterium are injected as blips, in #53015 in the after-puff the deuterium flux is stopped and a low Ar flux is continuously puffed, with a total injected level higher than in shot #52136.

Of particular interest is the analysis of shot #53548, in which deuterium is puffed during the whole plasma discharge. In this shot a relatively stationary phase is observed with high  $\Gamma$  ( $> 60\%$ ) and hollow radiation profiles. During this phase, an actual radiative mantle seems to have been established, with a significant increase of the radiation at the edge. Transport parameters similar to those of shot #53015 allow the fitting of the experimental data, but a significant neutral deuterium ( $4 \cdot 10^{15} \text{ m}^{-3}$  at the plasma edge) has to be added to match simultaneously the evolution of the experimental signals, the  $\rho$  ratio for carbon ( $\geq 5$ ) and the emission spectrum. As an example, fig.5 shows the time evolution of the line-integrated SXR signal measured on a central chord compared with the simulation. The emissivities in the figure are normalized, however in absolute terms the agreement is within a factor of two, i.e. well within the uncertainty in the absolute calibration of the diagnostic.

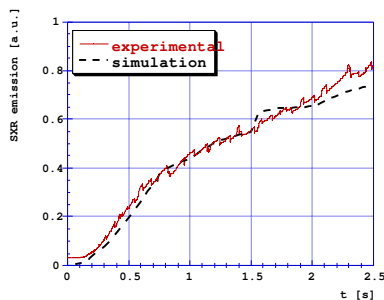


Fig. 5 :time evolution of the central soft X-rays signal

The presence of neutrals (associated with the continuous  $D_2$  puffing and consistent with a higher level of  $D_\alpha$  and  $Ly_\beta$  emission) reduces, via the charge-exchange processes, the average degree of ionisation of Ar at the edge, thus enhancing the edge

radiation (fig.4). So, on the one hand, for the total argon density a profile similar to that found for shot #53015 is calculated, as shown in fig. 3, and, on the other hand, a more hollow radiation profile, corresponding to an higher edge radiation, is obtained. Fig. 4 compares the experimental Abel-inverted profiles of the bolometer data and the related simulations for shots #53548 and #53015.

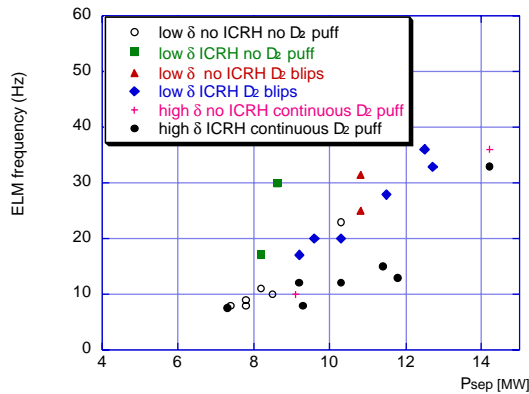


Fig. 6: ELMs frequency vs the power at the separatrix, calculated during the stationary phase as  $P_{tot} - P_{rad}$

**ELMs and confinement.** Since ELMs are related to the overall confinement of impurities their behaviour has been analysed in the good confinement phase of the three above mentioned scenarios. It appears that Ar injection mitigates the power per ELM to the targets [4] and reduces the ELM frequency, although the latter shows the usual proportionality with the power at the separatrix of type I ELMs and decreases with increasing triangularity (see fig 6). In two of the three scenarios studied the ELM frequency does not

depend on the mixing of NB and ICRH heating. The two shots #53015 and #53018 (low  $\delta$ , only Ar injection in after-puff) may suggest a beneficial effect on the ELM frequency of the ICRF heating. Also, it is worth noticing that the highest ELM frequencies are correlated with discharges at the highest values of  $T_e(0)$ .

Attempts have been done to identify a simple relationship between confinement and radiation pattern in the previous discharges. Not surprisingly, a different behaviour from case to case is found: the shots have different  $T_e$  and  $n_e$  as well as different magnetic configurations, while the radiation depends on all of these parameters.

**Conclusions** Two are the main results of the impurity transport analysis of the high performance Ar seeded JET discharges. When a moderate amount of ICRF central heating is applied the beneficial effects on preventing the central plasma cooling and the related pinch velocity outward directed seem to favour the formation of hollow profiles of Ar ions. The addition to ICRH to a continuous D<sub>2</sub> puffing in high  $\delta$  discharges results in an enhanced radiation at the edge due to the contribution of charge exchange processes. In this condition, the lower ELM frequency does not prevent the maintenance of high confinement values. These observations lead to the establishment of scenarios in which high performances are fully compatible with low central  $Z_{eff}$  and efficient power exhaust.

## References

- [1] Ongena, J., et al., Phys. Of Plasmas, 8, 2188 (2001)
- [2] Nave M.F.F., et al., "Sawtooth and Impurity accumulation control in JET radiative mantle discharges", this conf.
- [3] Mattioli M., et al., Jour. of Physics B, 34, 127 (2001)
- [4] Jachmich S., et al., "Influence of impurity seeding on ELM behaviour and edge pedestal in ELMy H-mode discharges", this conference